Slow spreading with a large contact angle on hygroscopic materials

Elisa Julien, Shmuel Rubinstein, Sabine Caré, Philippe Coussot

Cite this article :

E. Julien, S. Rubinstein, S. Caré, P. Coussot
Slow spreading with large contact angle on hygroscopic materials
https://doi.org/10.1039/D3SM00229B

Paper submitted to Soft Matter
Submitted: 21 Feb 2023
Accepted: 15 Apr 2023
First published: 17 Apr 2023

Contact: philippe.coussot@univ-eiffel.fr

Slow spreading with large contact angle on hygroscopic materials

E. Julien[1,2], S. Rubinstein[3], S. Caré[1], P. Coussot[1]

[1] Lab. Navier, Ecole des Ponts, Univ Gustave Eiffel, CNRS, 77420, Champs sur Marne, France
[2] Experimental Soft Condensed Matter Group, School of Engineering and Applied Sciences, Harvard University, Cambridge, MA, USA
[3] The Racah Institute of Physics, Faculty of Science, Israel

Abstract: Water transfers in wood play a major role during the life time of timber structures but the physics of the different various processes involved, such as wetting and imbibition, is not fully understood. Here we show that the angle of contact of a water drop placed in contact with air dry wood surface is initially larger than 90°, then the drop slowly spreads over the surface, while the apparent (macroscopic) contact angle decreases down to a few tens of degrees. We show that similar results are obtained with a model material, i.e. hydrogel, as soon as a perturbation is induced onto the line of contact. We demonstrate that for the gel the initial large apparent contact angle results from a strong deformation of the gel in a thin softened region below the line of contact resulting from the fast diffusion of water and swelling of this region. This phenomenon ensures a real (local) contact angle close to zero. The spreading then results from the progressive diffusion of water at farther distance and successive perturbations of the line of contact when the drop enters in contact with small liquid droplets dispersed along the surface (residues of the chemical reaction during gel preparation). It is suggested that a similar effect occurs for the water drop over a wood surface and explains the large initial contact angle and slow spreading: the line of contact is initially pinned thanks to a wood surface deformation resulting from wood surface swelling due to water absorption, thus leading to a large contact angle; it will then unpin when the local conditions have changed as a result of water diffusion at further distance, allowing for a small displacement up to the next pinning point and so on.

1. Introduction

Various materials such as cotton, paper, sugar, some salts, etc, are hygroscopic, i.e. they can attract (absorb) water molecules in their solid structure. In the field of construction, the hygroscopicity of wood, i.e. its ability to absorb water in cell-walls from vapor, is useful as it allows to regulate ambient humidity, but the swelling or shrinkage associated with water, i.e. the so-called bound water, absorbed inside the solid structure (cell-walls), can also induce physical or mechanical damages to the structure [1-3]. Woods also obviously absorb liquid water, but the cell-wall behavior and its impact on liquid transport when liquid water comes in contact with some wood surface are less clear. Such a situation is encountered during the impregnation of wood partially immersed in a liquid, painting or wood treatments, and in living wood at least partially filled with sap (essentially made of water). In such a case the liquid is expected to spread spontaneously over the solid

surface. The emerging question is that of (liquid water) wetting properties of a hygroscopic material.

Many works attempted to determine the contact angle of water on wood and two original effects were observed: i) a progressive decrease of the contact angle in time [4-8], and ii) a large difference between advancing and receding contact angles. It was suggested that the former effect (i) could be due either to the wood surface roughness or the absorption of water in the porous structure [5, 8-9] but no clear explanation was provided. The latter effect (ii) (large advancing/receding angle hysteresis) was considered to be due to the surface roughness [10]. Various other physico-chemical effects are suspected to play a role in the wetting properties [11-12]. It was also suggested that the strong difference between the advancing and receding contact angle has been so far too often neglected by people in the attempts to quantify interfacial energies [13], and that the non-equilibrium nature of wetting of water on wood should be taken into account in the theoretical interpretations of data [11]. Finally, in practice, it is generally considered that some "equilibrium" contact angle [8, 14] is *the* contact angle, an approach which neglects possible pinning effects.

Wetting properties may also be tested from imbibition tests, i.e. the penetration of liquid through the structure with capillary effects as the driving force. In that case it was shown that in hardwood the apparent contact angle in vessels, i.e. the contact angle measured from the droplet shape at the vessel scale, appears to strongly vary depending on whether the wood cell walls are saturated (in that case the contact angle is around 30°) or partially saturated (in that case the contact angle is around 90°) with bound water [15]. This effect was also observed with a model wood (in terms of hygroscopicity), i.e. a hydrogel. For both material types this phenomenon is associated with a strong slowdown of the imbibition dynamics, typically by several orders of magnitude of time [16]. It was then suggested that the wetting properties change with the water content of the gel [15-17], which evolves as a result of water diffusion beyond the line of contact. However, the origin of the different contact angle values remain unclear. A similar complexity emerges from observations by x-ray computed tomography images of water in wood lumen during drying: the liquid apparently dewets the cell-walls which are absorbing water [18], and various contact angles are then observed in the lumen [19].

Thus, there is a need to understand these particular wetting properties of wood, and distinguish the main effects among the various factors possibly playing a role (porosity, bound water absorption (hygroscopicity), roughness, presence of extractives). Here we intend to understand the origin of these different results, by focusing on the behavior of a droplet put in contact with the wood surface. We show that as soon as the wood is not saturated with bound water the initial contact angle is large, but then the drop slowly spreads over the surface while the contact angle decreases. From further tests with a model hygroscopic material (a hydrogel) leading to similar observations, we demonstrate that the line of contact of the drop is rapidly pinned, due to the surface deformation induced by water diffusion in the gel. The line of contact can nevertheless be unpinned, allowing the drop to slowly spread, if some effect tends to destabilize the line.

2. Materials and methods

Materials

Samples of various wood species (softwoods: fir, and hardwoods: poplar, oak and ash) were collected in Seine-et-Marne region (France). They were sawn along the anisotropic directions of wood (longitudinal L, Radial R and Tangential T) (see Figure 1a) and come from the inner part of the trunk (heartwood). Wood structure is essentially made of elongated hollow cellular units directed along the direction of the stem (called longitudinal direction), and along which a liquid (i.e. free water) can move in lumens (pores), surrounded by a solid structure able to adsorb water (i.e bound water) [18, 20]. Hardwoods and softwoods exhibit different detailed internal structures. Hardwoods are basically made of long (hollow) dead-end vessels whose diameter ranges from a few tens to about one hundred of microns depending on species, in a solid structure containing elongated enclosed fibers, which are cavities with a radius around a few microns able to store

some free water. Softwoods are essentially made of successive tracheids (diameter around 20-30 microns) in a solid structure. These tracheids are elongated channels, possibly connected by open or closed bordered pits preferentially located in earlywood. The axis of tracheids, vessels and fibers is the longitudinal one and corresponds to the main direction of the transfer of liquid water. The structure also contains rays, which are cells parallel to the radial direction, but their contributions to the transfer of liquid water may be neglected. Thanks to this structure water drops put on the RT plane tend to be rapidly absorbed in tracheids or vessels perpendicular to this plane, possibly with the help of absorption of bound water in the structure. In the tests discussed in this paper the droplets are put on the LR plane, which is essentially parallel to tracheids or vessels/fibers, which a priori precludes such fast capillary imbibition. Indeed, the penetration of free water perpendicularly to this surface (direction T), if any, is very slow, since the porous network is not connected in this direction or the apertures of the connections, i.e. pits between neighbouring vessels or tracheids, are tiny. The wood samples were taken at random places in the stem. The surface for the test was then planed. Under these conditions the resulting roughness of this surface corresponds to the internal wood structure, i.e. it is of the order of the vessel or tracheid diameter (see Fig.1b,c).

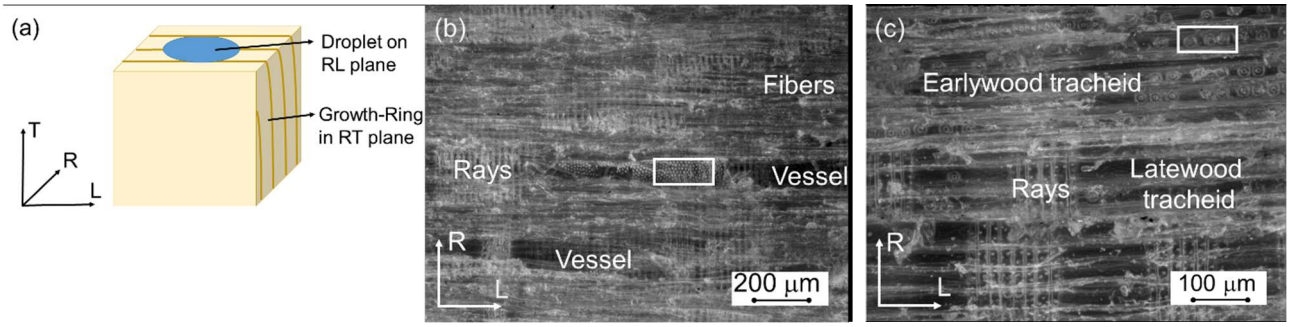

Figure 1: (a) Scheme of wood sample related to its anisotropic structure and its RL plane for the study of the droplet absorption (see text). Wood RL plan surface from optical microscopic analysis: (b) poplar; (c) fir. For (b) and (c), the plugin of FIJI 'Stack Focuser' was used to obtain a "focused" image from a stack of images corresponding to different focal planes (i.e., at different heights), depending for (b) on the diameter of vessels and for (c) on the diameter of tracheids. Microstructure: (b) Vessels and fibers are parallel to the L –axis, (c) Earlywood and Latewood tracheids are parallel to the L-axis, and in both cases Rays are parallel to the R-axis. Pits between two neighbouring vessels (b) or two earlywood tracheids (c) are indicated with a rectangle.

Hydrogels were formed from a solution of poly(ethylene glycol) methacrylate average Mn 500 (PEG methacrylate) (23.4 %wt), and poly(ethylene glycol) diacrylate average Mn 700 (PEG diacrylate) (2 %wt) in demineralized water (72.3 %wt) with a radical initiator, Ammonium persulfate at 5 wt% in water (1.15 %wt) and a catalyst, N,N,N',N'-Tetramethylethylenediamine at 10 wt% in water (1.15 %wt). All chemicals were purchased from *Sigma-Aldrich*, USA. The solution is poured in a cylindrical mold made in polyvinyl chloride (PVC) or poly(methyl methacrylate) (PMMA). The polymerization is finished after 30 min and the hydrogel can be easily unmolded as it slips along the solid surface. After this preparation we used the gel in two possible states: either as it, or after rinsing its surface with distilled water. In the latter case the surface appeared smooth at our scale of observation (see Fig. 2b) while, in the former case, small droplets with a diameter smaller than 20 microns appear at the free surface (see Fig. 2a). These droplets do not evaporate, so they are likely formed by a residual solution of the chemical process. No simple means appear to get further information on the components of these droplets, but this is not a problem within the frame of our study since we only deal with their directly observable properties.

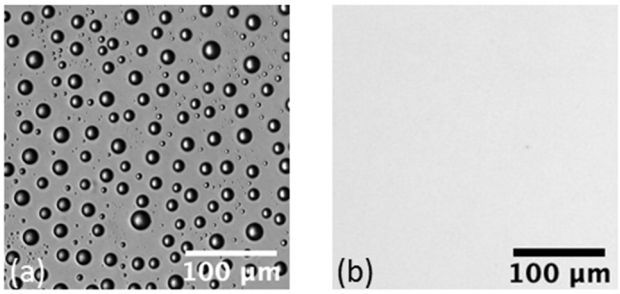

Figure 2: Aspect of the gel surface through optical microscopy imaging: (a) after the preparation; (b) after further rinsing.

The amount of bound water in wood is expressed as the moisture content (MC), i.e. the bound water to wood dry mass ratio. The MC varies with the relative humidity (RH). It tends to the FSP (Fiber Saturation Point), i.e., the maximum bound water content, when RH tends to 1 (see Appendix 1). Free water can be at equilibrium in contact with wood only when MC has reached the FSP. This means that as long as the MC is below the FSP, some small amount of liquid placed in contact with wood is expected to be progressively absorbed and the amount of bound water will increase leading to wood deformation [15]. For the hydrogel, the water concentration, i.e. the water to whole sample mass ratio, significantly varies with the relative humidity (RH), which induces large differences of the apparent volume as a function of RH. Moreover, as for wood, liquid water placed in contact with a gel sample prepared at a RH below 1 will penetrate it as long as the gel concentration is below a critical value. A complication with our gel is that this critical concentration (90%) is larger than that at which the gels have been initially made (74%). This nevertheless does not affect our analysis of the processes as the spreading properties are analogous on gels of concentration larger than 74%, which we call indifferently "saturated conditions". After its preparation each sample is placed in a desiccator in which the air is maintained at a fixed temperature (22°C) and a constant RH imposed by a saturated salt solution. The sample is then used when equilibrium is reached, the MC being given by the sorption curve (see Appendix 1). Simple compression tests for deformation up to 10% allowed to estimate the Young modulus (E) at 0.2 MPa for the gel at equilibrium with 50% RH, and 0.06 MPa for the saturated gel.

Set up

Figure 3 shows a scheme of the experimental set-up. A drop of liquid, usually 10 ± 2 µl of water is deposited on top of the wood RL plane or gel sample with a syringe and is filmed sideways with a 7.4 x 7.4 µm/pixel spatial resolution camera (acquisition frequency 15 fps). Water evaporation from the droplet was limited by placing the whole system in a box in presence of a water bath inducing a high RH. From tests made on a non-porous solid surface we checked that over the duration of the experiments (typically less than 30 min) the water uptake from (or release through) vapor by the gel was negligible.

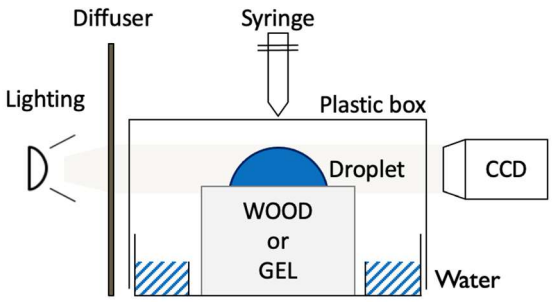

Figure 3: Scheme of the experimental set-up.

Imbibition in bulk hydrogel

We also measured the dynamics of absorption of water in the gel under simple geometrical conditions. A long cylindrical piece of hydrogel is immersed in a water bath at initial time. We then follow the volume of the sample by measuring the diameter of the cylinder over time. Due to the large aspect ratio of the sample (length to diameter ratio larger than 10) we expect the water penetration to be essentially in the radial direction. A similar test was recently used to estimate the dynamics of penetration of oil in oil-based gels, and more particularly the value of a "pseudo-diffusion" coefficient [21]. Here, we consider a standard diffusion process through a cylinder with a diffusion coefficient (D) of water in the gel. Under the (rough) assumption of a constant cylinder diameter we can fit the diffusion coefficient value in the theoretical expression for the entered volume vs time curve expression (see Appendix 2), which gives $D \approx 2.3 \times 10^{-11}\ \mathrm{m}^2\ \mathrm{s}^{-1}$.

3. Results and discussion

Drops on wood RL surface

Let us consider a wood sample prepared at a MC below the FSP. In that case the wetting characteristics have remarkable specificities. When a water drop is put in contact with a horizontal wood surface (RL plane), initially the apparent contact angle is very large, around 120°. Then the drop spontaneously slowly spreads during a few hundreds of seconds and the contact angle significantly decreases (see Fig. 4). These results are qualitatively consistent with previous observations [4-8], but here we provide detailed data concerning the drop characteristics over time. The spreading mainly develops along the longitudinal direction and remains much more limited in the perpendicular (R) direction (see Appendix 3). After some time, the spreading slows down and finally stops; this corresponds to the plateau in the spreading curve of Figure 4. In this second regime the drop volume also starts decreasing, either due to evaporation, absorption in the solid or flow through the porous structure. In the following we focus on the first regime, for which the liquid volume remains approximately constant. Note that in fact, according to the analysis below, in this regime there should be some slight absorption of water (in the form of bound water) in the structure, but the corresponding absorbed volume appears to be small compared to the current drop volume. Also note that we define the initial time as the time for which we get the first image for which the liquid is in contact with the gel. Thus, the uncertainty on the initial time is in the order of time between two successive images, i.e. 0.07 s. In any event, even with a larger frequency of acquisition it would be difficult to distinguish (i) the stage of development of the contact between the droplet and the gel surface (which also depends on the way the droplet is approached to the gel) from (ii) the initial stage of spreading. We also tested droplets of surfactant (sodium dodecyl sulfate)-water solutions but no significant impact was noticed, i.e. no change of the contact angle and spreading characteristics. As a consequence, we do not expect any effect of such a surface aging such as that described in [22] due to impurities.

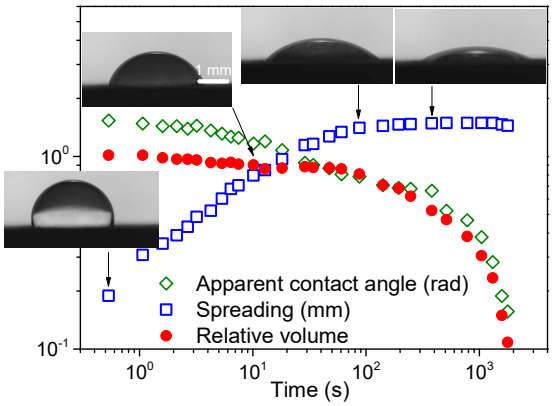

Figure 4: Water drop spreading along the direction L over a horizontal wood (fir) RL surface (prepared at 25% RH). Evolution of liquid drop characteristics in time: spreading length (diameter increase from initial value), relative volume (current to initial volume ratio) and apparent contact angle. Insets show the aspect of the drop at different times. Qualitatively similar results are obtained for the other wood types tested in this work.

The same qualitative features, i.e. slow spreading over a significant distance then apparent stoppage, were observed for different wood types (see Appendix 4), i.e. with hardwood and softwood which have different structures (see Materials and methods). This shows that this slow spreading with a large contact angle is a general phenomenon intimately linked to some common characteristics of woods. Note that likely due to the heterogeneity and variability of these systems, the results obtained for a given wood are significantly scattered: for example, for pine the dynamics varies by a factor about 10 depending on tests (see Appendix 4).

To further confirm the originality of this slow spreading observation we can compare it with the prediction of the standard Cox-Voinov approach [23-24]. This leads to express the capillary number as a function of the contact angle (θ), which may be approximated as $\left(\theta^3 - \theta_{eq}{}^3\right)/9\,\mathrm{Log}(L/a)$ [25], in which θ_{eq} is the contact angle at equilibrium, L the drop size and a a cut off length of the order of 1 nm. On the other side the capillary number expresses as $\mu V/\sigma$, in which μ is the water viscosity, σ the surface tension and V the spreading velocity. Here, from the data of Figure 4, we deduce that V decreases from 0.05 mm/s to 0. This implies that the maximum value of the capillary number is in the order of 10^{-6}. Such a value can balance the above function of the contact angle only if this angle is very close to zero (here in the order of 2°) or very close to its equilibrium value, which does not correspond at all to our observations. This shows that the observed spreading does not follow a process based of a competition between viscous and capillary effects.

Whereas wood is generally considered “hydrophilic”, which seems justified by its ability to absorb vapor, the large values of contact angles systematically obtained in early times suggest that it is in fact hydrophobic. Considering the complex, rough, structure of the wood surface one might consider such a large contact angle as due to the roughness of the surface, but the effect of roughness is generally [26] to increase the hydrophilic or hygroscopic nature of the surface. So, if the “true” contact angle was smaller than 90° the roughness would tend to decrease it further. Thus, the roughness cannot a priori induce such a large contact angle if the contact angle over the smooth surface is very small.

Under these conditions, one possibility is that the contact angle observed is in fact an apparent contact angle resulting from a pinning of the line of contact at some position during the drop deposit over surface: the line of contact being fixed the apparent contact angle just results from the volume of liquid drop taking approximately a spherical shape (due to the Laplace pressure drop, possibly with some slight gravity effects). At this stage we have nevertheless no explanation for this possible pinning. Moreover, if such a pinning indeed occurs it is particularly surprising to observe that the line of contact slowly advances, as this is a priori

in contradiction with the assumption of pinned contact line: the displacement is necessarily associated with some unpinning. Even more remarkable is the fact that, at our timescale of observation, the fluid continuously advances over the plane, without significant stick-slip effects as expected from unpinning events. This implies that something only progressively changes in time around this contact line. This change likely finds its main origin in the water absorption capacity of the wood, which progressively develops in time. However, during the first regime, i.e. the spreading phase, the decrease of the liquid volume is negligible (see Fig. 4). This means that the main open porosity (in the direction T) of the wood has not been significantly invaded by the liquid, in the form of free water, during this stage. Following our recent observations of imbibition of wood [15-17] showing that bound water penetrates faster than free water, it is likely that, here, in the first regime, most absorbed water is in the form of bound water in the cell-walls.

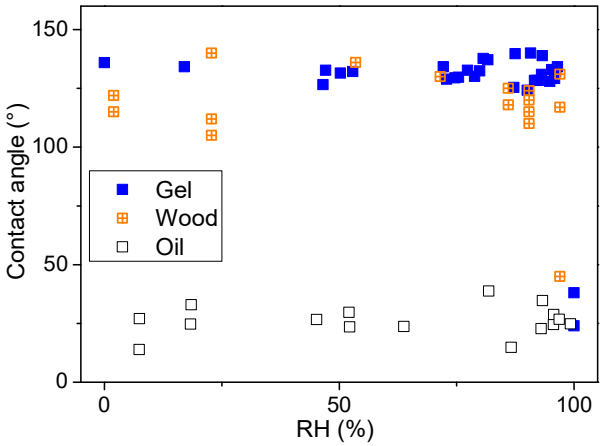

Figure 5: Initial contact angle of water over a wood (fir) or hydrogel non rinsed surface, and of oil on hydrogel, as a function of the RH at which the sample (gel or wood) has been prepared.

To further check the role of bound water absorption in the measured angle of contact and drop spreading, we carried out tests with samples prepared at different RH values, associated with various MC values. No significant change was observed (see Figure 5) as long as the initial MC is below the FSP. In contrast, when the sample has been prepared at a MC approaching the FSP, the initial angle of contact drops to a low value and the droplet rapidly spreads over the wood surface (see Figure 6). Furthermore, a low viscosity oil droplet also rapidly (typically in less than one second) spreads over the wood surface (whatever its MC) with a small contact angle. These different observations further confirm the major role of the bound water absorption on the initial large contact angle and drop spreading.

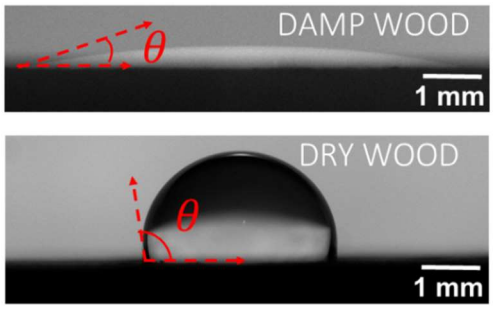

Figure 6: Water drop on a (fir) wood surface, either prepared at 100% RH (top) (“damp”) or at 25% RH (bottom) (“dry”): initial contact angle.

Drops on hydrogel surface

In order to confirm this analysis and further study the origin of this phenomenon, we repeat these experiments of drop deposit with a cleaned hydrogel (see Figure 2b). In that case the drop exhibits a large initial apparent contact angle (see Figure 7) but does not significantly spread. For hydrogels we can directly compute the interfacial energies between the different phases, which a priori makes it possible to predict the contact angle from the Young-Dupré equation [26]. Since water is the polymer solvent, as long as the gel is at equilibrium and not almost dry, the free surface of polymer chains is surrounded by water molecules. Thus, the gel-air and water-air interfacial energies should be close (i.e. $\gamma_{GA} = \gamma_{WA} = \sigma \approx 0.07 \text{ N m}^{-1}$, with indices *A* for air, *G* for gel, *W* for water) and the gel-water interfacial energy should be equal to zero ($\gamma_{GW} = 0$). It follows that the spreading coefficient, i.e. $S = \gamma_{GA} - (\gamma_{GW} + \gamma_{WA})$, is equal to zero, which implies that a contact angle equal to zero is expected at equilibrium, whatever the gel concentration may be, and not a large apparent contact angle as observed in our tests of water drop deposited over the gel surface.

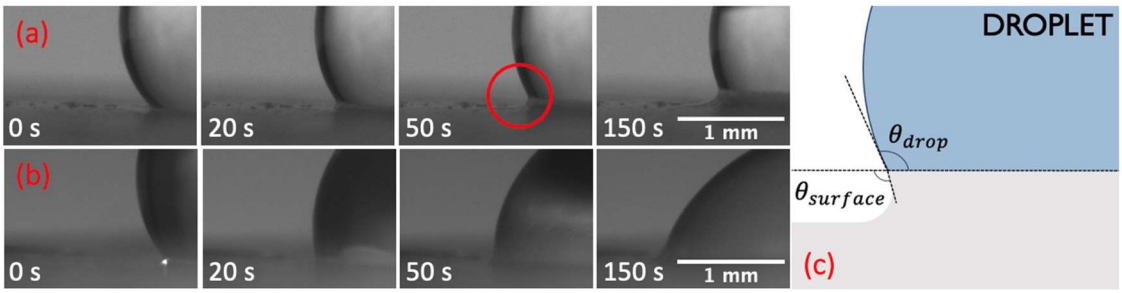

Figure 7 : (a) Local aspect of the foot of a droplet at different times after placing it on a gel surface (prepared at 50% RH): (a) rinsed gel, (b) non-rinsed gel. The red circle shows a typical region of deformation of the gel. (c) Scheme of the principle of gel swelling around the contact line, allowing for a large apparent contact angle (θ_{drop}), whereas the effective contact angle (at a local scale), is close to zero, i.e. $\theta_{surface} \approx \theta_{drop}$.

Actually, a similar effect, i.e. large contact angle, was already observed for water or water-surfactant drops put on agar gel surfaces [27], but the question of its origin remained open. On the other side a fast spreading associated with a low contact angle was observed on rough (fractal) agar surfaces [28]. For another hydrogel type, Kajiya [29] and Boulogne [30] also observed a relatively large initial contact angle (but smaller than 90°) and the line of contact remains pinned. In those cases [29-30], no spreading was observed and during some initial period the local contact angle ($\theta_{surface}$) was considered to be larger than the angle formed by the substrate (θ_{drop}) (see Figure 7c) and the substrate progressively deforms; in the next period we have $\theta_{surface} \approx \theta_{drop}$ and the contact line recedes while the drop volume decreases [29].

Here a similar effect occurs: we can see the gel swelling and deformation from the very first times, allowing to maintain a rather small contact angle between the drop surface and the gel surface. At the very beginning it is difficult to have precise information on the local contact angle (i.e. with respect to the gel surface at the contact point), but in the next stages it becomes clear that the tangents to the liquid and solid surfaces are very close at the point of contact (see Figure 7a at 50 and 150 s), as represented in the scheme of Figure 7c. Actually, even if it is more difficult to appreciate the phenomenon from the pictures when the substrate deformation is small (i.e. at short times), it seems that we have at any time $\theta_{surface} \approx \theta_{drop}$.

Note that such a phenomenon does not seem to be solely explainable by the “soft” (elastic) behavior of the gel which would deform under the action of capillary effects, as considered in a series of experimental and theoretical approaches [31-34]. Indeed, here we can consider that the gel would undergo a deformation γ larger than 1 in the region around the line of contact. Then the elastic stress is in the order of (or larger than)

$E\gamma$, i.e. larger than several tens thousand of Pascals, while the capillary stress is σ/R, in which R is the droplet size, σ the surface tension. Here, since R is in the order of 2 mm, we have $\sigma/R \approx 35$ Pa<<$E\gamma$. Thus, capillary effects alone cannot be at the origin of the significant deformation undergone by the gel around the line of contact. This deformation rather finds its origin in the fast penetration of water in a thin region of the hydrogel in contact with the drop, which induces the gel swelling. As it swells the gel then likely adjusts its shape to preserve a local contact angle around zero. The phenomenon is nevertheless rather complex, as it results from some fast initial spreading on the drop and simultaneously water diffusion into the hydrogel then swelling of the gel. We can suggest that a thin water film tending to advance over the gel would rapidly penetrate the gel by diffusion, faster than it can advance; then the gel locally somewhat swells. At some point, this swelling would allow the shape of the substrate to get $\theta_{surface} \approx \theta_{drop}$, thus stoppage and pinning.

This explanation is supported by the observation that, on the contrary, for a fully saturated gel, i.e. which cannot absorb more water and thus cannot swell, a water drop exhibits a small contact angle and rapidly widely spreads over the surface (see Figure 5). Thus, the contact angle drops to zero when no swelling is possible. In the same way, for an oil drop of viscosity similar to that of water, the contact angle is much lower than 90° (see Fig. 5), and this oil widely spreads in a time orders of magnitude shorter than it takes the water drop to spread on an unsaturated gel, whatever the gel concentration. This confirms that standard wetting properties are recovered in the absence of gel swelling (here the oil in any case, and the water over a saturated gel, are not absorbed by the gel).

Thanks to this swelling the line of contact is rapidly pinned after the first contact, which is at the origin of the large apparent contact angle value. In fact, we have a confirmation of this pinning by looking at the advancing and receding contact angles. We measure the advancing contact angle by progressively injecting water in a drop just placed on the gel surface. The advancing contact angle then remains approximately constant (see Fig.8a) and equal to the initial angle of contact observed after pouring the drop. Thus, the initial contact angle observed when depositing the drop in our initial experiment may be considered as an advancing contact angle. If we now withdraw the liquid from the drop just placed on the horizontal solid surface, the line of contact does not recede (see Fig. 8b), it remains pinned, so that the apparent angle of contact decreases to zero as the drop volume decreases to zero.

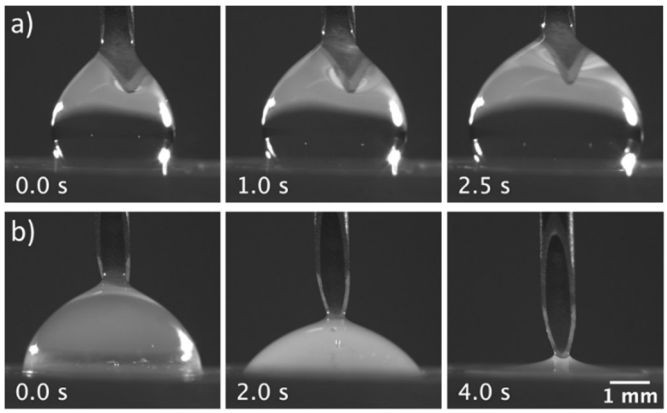

Figure 8: Views at successive times of (a) the progressive injection of water in a drop just placed in contact with a hydrogel surface (RH=50%) and (b) the progressive withdrawal of water from the drop.

Origin of the large contact angle and slow spreading on wood surface

An effect similar to that above described likely occurs in the very first time of contact between the water drop and the wood surface, due to the diffusion of water inside the cell-walls of the wood and the resulting swelling of its surface layer. Thus the line of contact is pinned. Under these conditions, more intriguing is the slow drop spreading observed afterwards. Here we suggest that this occurs as a result of a perturbation of

the line of contact: the water diffusion in the wood region, just beyond the line of contact, would lead to an uneven deformation of the rough wood surface, inducing successive slight modifications of the contact line and thus inducing successive steps of slight spreading. In order to test this idea we need to modify the gel surface, which is clean and smooth for a rinsed gel. We can instead use a non-rinsed gel, whose surface is covered by small droplets of liquid (see Fig.2a) that can play a role analogous to that of the wood unevenness and the resulting successive perturbations of the contact line as it advances over the gel surface.

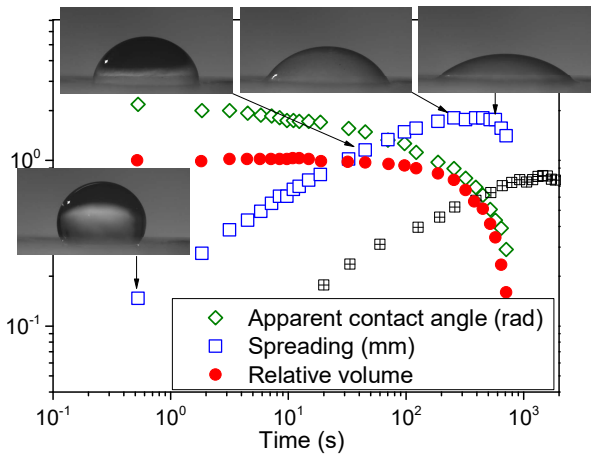

Figure 9: Water drop spreading over a horizontal surface of a non-rinsed gel (prepared at 50% RH). Evolution of liquid drop characteristics in time: spreading length (i.e., diameter increase from initial value) (blue squares), relative volume (i.e., current to initial volume ratio) (red circles) and contact angle (green diamonds). Insets show the aspect of the drop at different times. The spreading length for a rinsed gel (same water concentration) is also shown (cross-squares).

In that case, when placing a water drop on the gel surface, we now obtain results very similar to those obtained with wood (see Figure 7b and Figure 9): (i) large initial contact angle then (ii) slow spreading over the surface, and finally (iii) penetration of the water in the gel. Also, as for wood, we do not observe any significant impact of the initial water concentration of the gel: in particular, an almost constant value of initial contact angle is observed in a wide range of concentrations (see Fig. 5). Moreover, again as for wood, when placed over a saturated hydrogel, a drop rapidly spreads over the surface with a small contact angle. At last note that when the spreading has stopped (iii), the evolution of the volume is mainly controlled by the absorption of water in the gel. This is a diffusion process basically similar to the experiment described in Appendix 2, but here the process is slightly more complex as it is a 3D diffusion from a finite surface.

Here we can follow the swelling of the solid surface which occurs immediately after the first contact and then progressively develops. Indeed, it results, due to some reflection and refraction effect on the swollen region, in the appearance and growth of a lighter region at the bottom of the drop (see the drop bottom region in the inset photo at 45 s in Figure 9). In fact, the real thickness of this region is much smaller than it appears when viewed from outside, as it can be estimated from the height of the non-spherical shape of the drop over the initial gel surface. In the final stage, this swelling has yielded a solid gel promontory above which the remaining liquid lies (see last inset image of Figure 9). However, since the line of contact continuously advances, a local deformation (due to swelling) of the gel around the line of contact is successively induced at another place, so that in contrast with the rinsed gel (see Figure 7a) it has no time to develop and remains rather small (see Figure 7b), except in the last stage when the progression has stopped. It remains that this local deformation allows the effective contact angle to be much lower that the measured apparent contact angle.

The difference in drop behavior on the rinsed and not rinsed gel surface likely comes from the presence of the small droplets of unknown liquid in the latter case (see Figure 2a). In that case, looking at the drop

spreading at a smaller scale we can see that these droplets are progressively included in the water drop (see Figure 10). The way these droplets are included in the water drop, either by mixing (miscible liquids) or by covering the drop surface (immiscible liquids), is not critical here and we will not discuss it further. The critical point is that the line of contact is continuously disturbed as it advances and encounters new droplets and so on. These successive perturbations are at the origin of its advance. After each step forward the line of contact encounters a new gel region, which rapidly swells, and a new provisional equilibrium would tend to be reached, soon destabilized when the contact line encounters other droplets at other points.

Note that the origin of the dynamics of the line of contact in that case is still unclear. Even if at each step the new position of the line of contact is dictated by the swelling of the gel, associated with the water diffusion, the progression cannot be readily related to the dynamics of the diffusion of water in the gel. Indeed, this would typically lead to a diameter increase as $4\sqrt{Dt}$, with D the diffusion coefficient found for water imbibition in a gel (see Materials and methods), but this predicts a much slower progression than observed. The drop spreading thus likely results from a complex coupling between water diffusion, swelling and frequency of perturbations of the contact line.

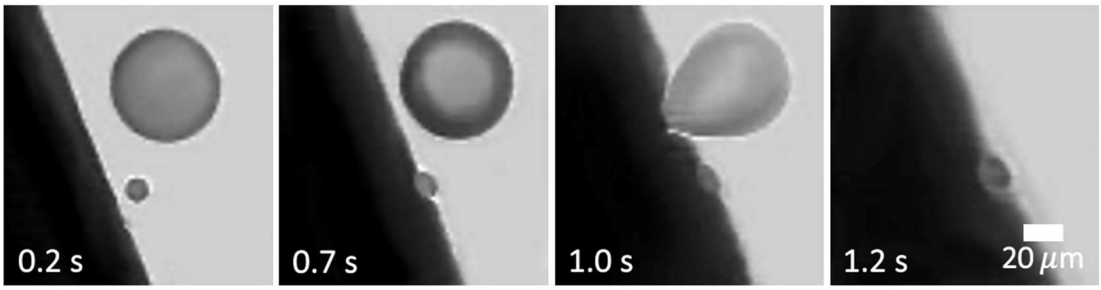

Figure 10: Successive upper views of a line of contact of a water drop (black) advancing on the surface of not rinsed gel (RH=50%) (white). We can see the behavior of two droplets (grey) of residual liquid in front of the line of contact: the largest one is immediately included in the water drop when it touches it; the smallest one is just deformed, remains in contact with the line of contact and is pushed by the drop.

Actually, the presence of these droplets allows to confirm that the gel is strongly deformed at the approach of the line of contact, to maintain a real contact angle of the water drop around zero. Indeed, it appears that depending on their size the droplets, when they reach the line of contact, behave differently (see Figure 10). Large droplets are immediately included in the water drop when they reach the line of contact, which means that they enter in contact with the water-air interface. In contrast, small droplets are just deformed and remain along the line of contact, and they are then displaced as the line of contact goes on advancing. This observation supports the above suggestion that the gel is strongly deformed around the line of contact so as to ensure a real local contact angle around zero, and the height of this deformation increases in time. Indeed, under such conditions, a droplet of size larger than this height can touch the drop surface, while a droplet of size smaller than this height will remain in the curved region of the gel. From statistics over a set of droplets we can draw a diagram showing the size of deformed or included droplets. The boundary between these two regions provides an estimate of the evolution of the height of deformed gel. We see that it increases in time (see Fig. 11). However, this height is at any time significantly lower than the height of the deformed region observed in the case of definitively pinned contact line, which is rapidly equal to a few hundreds of microns (see Figure 7a bottom).

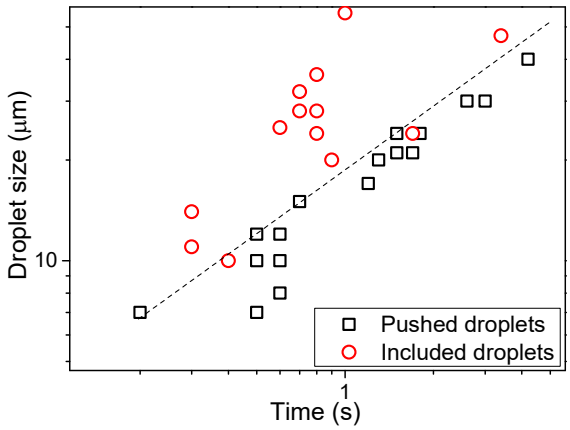

Figure 11: Size of the droplets of residual liquid as a function of time observed along the drop spreading in experiments with non-rinsed gel similar to that presented in Figure 9. The two types of behavior are distinguished: included (circles) or pushed (squares) droplets.

In order to explain our results we could also turn to the significant works concerning the displacement of the contact line of droplets lying on permeable rough surfaces, including complete reliable theoretical approaches taking into account the different phenomena [35-37]. However, in the current state, there appear to be several significant differences between our observations and the field of application of these previous descriptions: it is unlikely that there is a precursor film on our hydrogel, it would be almost immediately absorbed in the gel; with our smoothest (rinsed) surface there is no unpinning of the contact line until the full absorption of the drop in the gel; we essentially observe an advance of the contact line, while these works essentially describe its withdrawing due to water penetration in the substrate pores; the impact of rugosity in our case might be seen through the impact of the presence or absence of liquid droplets on the surface, but here this pseudo rugosity favors the contact line advance.

At last, we can remark that we could observe a significant difference of the dynamics of spreading when using a more concentrated gel than the one shown in Figure 9. At a concentration of 70% the spreading curve is quite similar to that obtained for a concentration of a few percent (at an equilibrium RH of 50%), but shifted towards lower time value by a factor about 4, i.e. the plateau regime for spreading starts around a time of 50 s (instead of 200 s) for the case shown in Figure 9. However, it does not seem so easy to find the explanation for such an effect. Indeed, a difference of initial concentration should not affect the timing of absorption, i.e. the distance of water penetration by diffusion reached after a given time is the same whatever the initial concentration (see Crank [38]).

4. Conclusion

Considering the similarity of their physical properties and the similarity of the behavior of water drops on their surface, it seems natural to consider that the explanation proposed for hydrogels applies to wood: the initial large contact angle results from the absorption of water as bound water in the solid structure of the material which forms a thin soft swollen region, deformed so as to have a limited local contact angle but a large apparent contact angle of the drop; the line of contact is then pinned, but will unpin when the local conditions have changed. In that case we expect that the destabilization is due to the fact that the wood surface roughness somewhat evolves as bound water penetrates it, so that the line of contact must continuously adapt its shape to this new local shape of the solid surface.

The control of the drop advance by the water diffusion and gel swelling is further illustrated by similar experiments over an inclined wood or gel surface. A water droplet now slowly spreads over the surface along the slope, and the downward contact angle progressively decreases (see Figure 12). In contrast, a drop of

dodecane, i.e. an alkane hydrocarbon liquid of viscosity (1.3 mPa.s) close to that of water, immediately exhibits a small contact angle and spreads downwards in a timescale shorter by several orders of magnitude than water (see Figure 12). For a drop size of a few millimeters, an estimation based on the competition between gravity and viscosity (see Appendix 5) predicts a displacement of the order of 1 cm over the first 0.1 s, which is quite consistent with our observation of dodecane on wood, but is several orders of magnitude shorter (of the order of 1 cm over the first 100 s) than the observations for water on wood. Thus, as for the displacement over a horizontal surface, the line of contact moves as a result of some destabilization effect, but its velocity is strongly limited and controlled by the swelling and deformation of the wood or gel occurring a step farther.

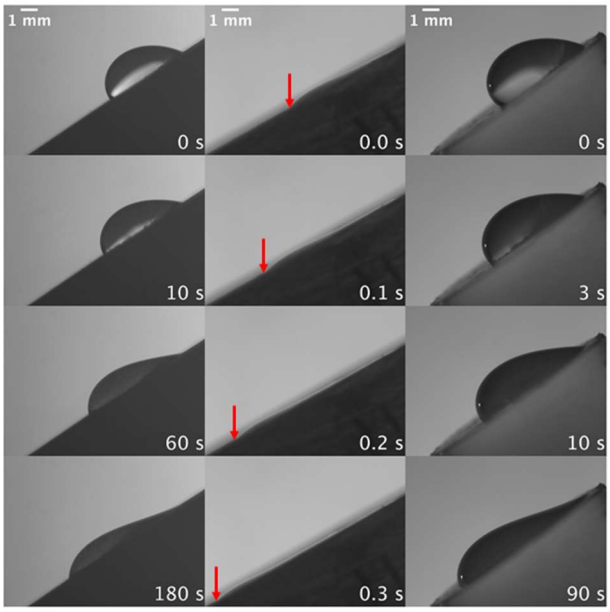

Figure 12: Spreading of a liquid drop poured over inclined surfaces: side views at different times for water on wood (left) or hydrogel (right), oil (dodecane) on wood (center) (fir wood). The red arrow indicates the position of the drop front for oil. All samples were prepared at 50% RH.

Although the physical process at a macroscopic scale can seem rather simple, the complete modelling of the process seems rather complex as it requires to take into account the 3D characteristics of the diffusion and the resulting deformability of the solid up to large deformation, along with the liquid volume in the drop.

As a particular consequence of this phenomenon, the wetting of such soft hygroscopic materials with water is strongly damped under usual conditions, and can develop spontaneously only when they are saturated with water. This is consistent with the observations of strong damping of capillary imbibition in wood and gel [16]. However, in these cases, the slow spreading continues until filling the vessels over several centimeters high. This is due to the fact that the water supply is not limited, so that the gel will ultimately become fully saturated at any distance from the initial contact.

Another consequence of our observations is that the angle of contact is not an intrinsic property of these systems, but a result of the liquid volume and the history of contact between the liquid and the solid surface. Thus, if we spread a drop of water with a tool over a wood or gel surface and then try to displace the liquid with the same tool, wherever it has been in contact with the gel the liquid remains in contact with it, i.e. no dewetting at all occurs.

Authors contribution: EJ, SR and PC conceptualized the experiments. SC and EL worked on the methodology. SC provided resources. Investigation and data analysis were carried out by EJ. SR and PC supervised the work. EL, SC, SR and PC took part to the manuscript writing.

Acknowledgments: We acknowledge fruitful discussions with François Boulogne, E. Lorenceau and Camille Duprat.

Appendices

Appendix 1: Sorption and desorption

After its preparation each sample is placed in a desiccator in which the air is maintained at a fixed temperature (22°C) and a constant RH imposed by a saturated salt solution, and the sample is weighted when equilibrium is reached (typically after 2 weeks). Various saturated salt solutions were used leading to different RH. Measuring the mass fraction of water at equilibrium for the different RH makes it possible to obtain the sorption isotherm of the material.

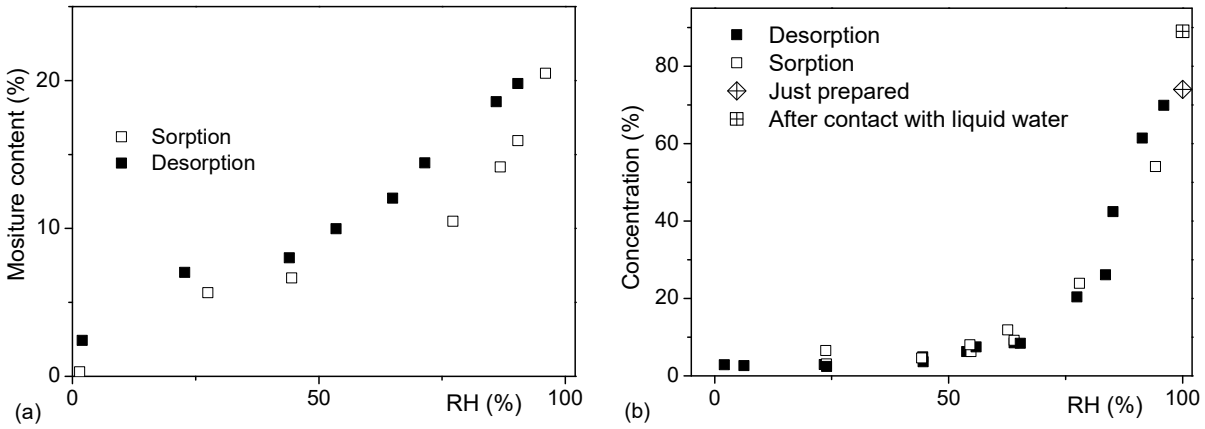

Figure 13: Sorption and desorption curves for the fir wood (a) and the gel (b). The cross-square symbol corresponds to a gel at equilibrium in contact with a liquid bath.

Appendix 2: Gel imbibition

The data for the imbibition of a gel cylinder immersed in water are shown in Figure 14. We fitted to the data the solution for simple diffusion through a cylindrical volume at a given initial concentration. A critical assumption here is that the diameter is constant and equal to the initial one. This obviously does not correspond to our case since the diameter reaches a final value (at saturation, here a concentration of 90%). The model predicts that the entered volume of water is given by

$$\Omega(t) = \Omega_{\max}\left[1 - \sum_{n=1}^{\infty} \frac{4}{a^2 \alpha_n{}^2} \exp(-D\alpha_n{}^2 t)\right]$$

In which $\Omega_{\max}$ is the maximum volume that can enter the gel, α_n is the nth root of $J_0(a\alpha_n) = 0$, in which J_0 is the Bessel function of the first kind of order zero, and a the cylinder radius. This model remarkably fits to the data (see Figure 14) despite our strong assumption on the diameter value. A full description of the mechanisms should take into account the poroelasticity of the medium [21]. However, the agreement with a simple diffusion model in a constant diameter cylinder whereas taking into account the diameter variations would lead to a significantly different prediction of the model, suggests that despite the sample swelling there is a physical analogy of the mechanisms with a simple diffusion in a constant diameter cylinder.

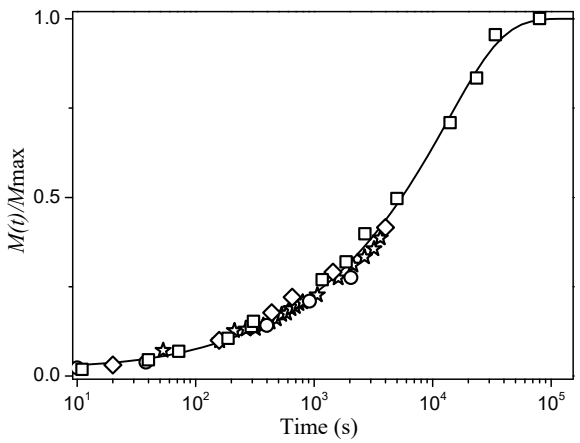

Figure 14: Water imbibition in a gel cylinder (initially dry) of initial diameter 2.8 mm. The different symbols correspond to different experiments. The continuous line is the model (see text) fitted to data by adjusting the diffusion coefficient value.

Appendix 3: **Drop spreading on wood: top view.**

Here we present a typical set of pictures of the spreading of a drop on wood (fir) taken from above (see Figure 14), illustrating the anisotropic spreading, i.e. larger in the L direction.

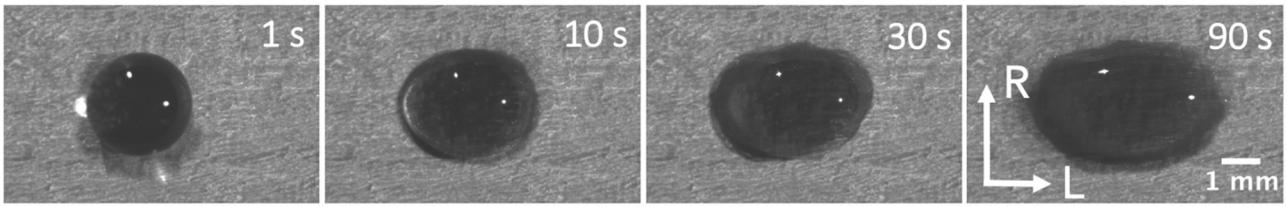

Figure 15: Water drop placed on wood: shape from above at different times during spreading.

Appendix 4: Drop spreading on different wood types

Here we present some data (see Figure 15) corresponding to the spreading of water drop on different wood types. Note that, as illustrated by different tests presented for the fir wood (see Figure 15), such data, obtained by deposits on different points of a wood sample surface, are only poorly reproducible. We believe that this is due to the roughness variations of the surface at the scale of the droplet, which strongly affect the initial contact and spreading. However the qualitative trends of the process, i.e. the slow spreading over a distance larger than 1 mm, are reproducible.

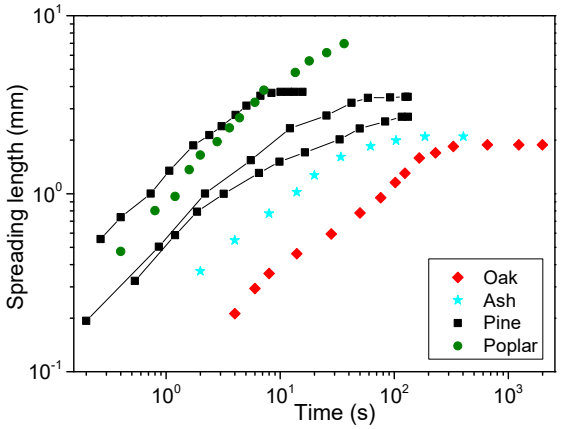

Figure 15: Water drop spreading along the direction L over different horizontal wood surfaces (prepared at 50% RH) (filled symbols): spreading distance (diameter increase from initial value) as a function of time.

Appendix 5. Spreading of a drop over an inclined plane

Let us consider the flow of such a drop along the slope for a pinned upper line of contact, as is apparently the case here (in fact a slight upward motion is observed, of a fraction of millimiter). Neglecting inertia and capillary effects, the spreading is governed by a balance between (a) the gravity stress, i.e. at first order $\rho g h \sin i$, where h is the typical thickness of the drop, ρ the liquid density, g the gravity and i the plane slope, and (b) the viscous stress, i.e. $\mu\dot{\gamma}$, in which $\dot{\gamma}$ is some gradient of velocity in the drop and μ the liquid viscosity. Here, for the sake of simplicity, we estimate $\dot{\gamma}$ by assuming a simple shear, so that $\dot{\gamma} \approx (1/h)\mathrm{d}x/\mathrm{d}t$, an assumption strictly valid when $h << x$, x being the position of the line of contact along the plane or equivalently the drop length. Taking into account that the liquid volume is constant (i.e. $xLh \approx \Omega$), we get after integration $x \approx \left(\rho g \Omega^2 \sin i / \mu L^2\right)^{1/3} t^{1/3}$. Typically, for a drop size of a few millimeters, this expression predicts a displacement of the order of 1 cm over the first 0.1 s, which could be consistent with our observation of dodecane on wood (see Figure 12), but is several orders of magnitude shorter (of the order of 1 cm over the first 100 s) than the observations for the water on wood.

References

[1] D. Kretschmann, Nature materials: Velcro mechanics in wood. Nature Materials, 2000, **2**, 775–776

[2] J.H. Van Houts, S. Wang, H. Shi, et al, Moisture movement and thickness swelling in oriented strandboard, part 1. Analysis using nuclear magnetic resonance microimaging, Wood Sci. Technol., 2004, **38**, 617–628.

[3] C. Silva, J.M. Branco, A. Camões, P.B. Lourenço, Dimensional variation of three softwood due to hygroscopic behavior, Constr. Build. Mater., 2014, **59**, 25–31

[4] C. Piao, J.E. Winandy, T.F. Shupe, From hydrophilicity to hydrophobicity: a critical review: Part I. Wettability and surface behavior, Wood and Fiber Science, 2010, **42**, 490-510

[5] C. Boehme, G. Hora, Water absorption and contact angle measurement of native European, North American and tropical wood species to predict gluing properties, Holzforschung, 1996, **50**, 269-276

[6] S.Q. Shi, D.J. Gardner, Dynamic adhesive wettability of wood, Wood Fiber Science, 2001, **33**, 58-68

[7] J.Z. Lu, Q.L. Wu, Surface characterization of chemically modified wood: Dynamic wettability?, Wood Fiber Science, 2006, **38**, 497-511

[8] M. Scheikl, M. Dunky, Measurement of dynamic and static contact angles on wood for the determination of its surface tension and the penetration of liquids into the wood surface, Holzforschung,

1998, **52**, 89-94

[9] E. Liptakova, J. Kudela, Analysis of the wood-wetting process, Holzforschung, 1994, **48**, 139-144

[10] M.E.P. Walinder, G. Ström, Measurement of wood wettability by the Wilhelmy method – Part 2 Determination of apparent contact angles, Holzforschung, 2001, **55**, 33-41

[11] S. Barsberg, L.G. Thygesen, Nonequilibrium phenomena influencing the wetting behavior of plant fibers, J. Colloid and Interface Science, 2001, **234**, 59-67

[12] W. Wang, Y. Zhu, J. Cao, W. Sun, Correlation between dynamic wetting behavior and chemical components of thermally modified wood, Applied Surface Science, 2015, **324**, 322-338

[13] M.A. Hubbe, D.J. Gardner, W. Shen, Contact Angles and Wettability of Cellulosic Surfaces: A Review of Proposed Mechanisms and Test Strategies, Bioresources, 2015, **10**, 8657-8749

[14] A. Laskowska, P. Kozakiewicz, Surface wettability of wood species from tropical and temperate zones by polar and dispersive liquids, Drvna Industrija, 2017, **68**, 299-306

[15] M. Zhou, S. Caré, D. Courtier-Murias, P. Faure, S. Rodts, P. Coussot, Magnetic resonance imaging evidences of the impact of water sorption on hardwood capillary imbibition dynamics, Wood Science and Technology, 2018, **52**, 929-955

[16] M. Zhou, S. Caré, A. King, D. Courtier-Murias, S. Rodts, G. Gerber, P. Aimedieu, M. Bonnet, M. Bornert, P. Coussot, Liquid uptake governed by water adsorption in hygroscopic plant-like materials, Physical Review Research, 2019, **1**, 033190

[17] D.M. Nguyen, S. Caré, D. Courtier-Murias, M. Zhou, P. Coussot, Mechanisms of softwood imbibition inferred from Magnetic Resonance Imaging, Holzforschung, 2021, **75**, 225-236

[18] M. Cocusse, M. Rosales, B. Maillet, R. Sidi-Boulenouar, E. Julien, S. Caré, P. Coussot, Two-step diffusion in cellular hygroscopic (plant-like) materials, *Science Advances*, 2022, **19**, eabm7830

[19] H. Penvern, M. Zhou, B. Maillet, D. Courtier-Murias, M. Scheel, J. Perrin, T. Weitkamp, S. Bardet, S. Caré, P. Coussot, How bound water regulates wood drying, *Physical Review Applied*, 2020, **14**, 054051

[20] J. Siau, *Transport process in wood* (Springer-Verlag, New York, 1984).

[21] P. Van de Velde, S. Protière, C. Duprat, Dynamics of drop absorption by a swelling fiber, Soft Matter, 2021, **17**, 6168

[22] A. Ponce-Torres, E.J. Vega, J.M. Montanero, Effects of surface-active impurities on the liquid bridge dynamics, Exp. Fluids, 2016, **57**, 67

[23] O.V. Voinov, Motion of line of contact of three phases on a solid: thermodynamics and asymptotic theory, Int. J. Multiphase Flow, 1995, **21**, 801-816

[24] R.G. Cox, The dynamics of the spreading of liquids on a solid surface. Part 1. Viscous flow, J. Fluid Mech., 1986, **168**, 169-194

[25] C. Monteux, Y. Elmaallem, T. Narita, F. Lequeux, Advancing-drying droplets of polymer solutions : Local increase of the viscosity at the contact line, EPL, 2008, 83, 34005

[26] P.-G. de Gennes, F. Brochard-Wyart, D. Quéré, *Capillarity and Wetting Phenomena: Drops, Bubbles, Pearls*, *Waves*, (Springer, Berlin, 2003)

[27] M. Banaha, A. Daerr, L. Limat, Spreading of liquid drops on Agar gels, European Physical Journal Special Topics, 2009, **166**, 185-188

[28] Y. Nonomura, Y. Morita, T. Hikima, E. Seino, S. Chida, H. Mayama, Spreading behavior of water droplets on fractal Agar gel surfaces, Langmuir, 2010, **26**, 16150-16154

[29] T. Kajiya, A. Daerr, T. Narita, L. Royon, F. Lequeux et L. Limat, Dynamics of the contact line in wetting and diffusing processes of water droplets on hydrogel (PAMPS-PAAM) substrates, *Soft Matter*, 2011, **7**, 11425-11432

[30] F. Boulogne, F. Ingremeau, L. Limat, H.A. Stone, Tuning the Receding Contact Angle on Hydrogels by

Addition of Particles, Langmuir, 2016, **32**, 5573-5579

[31] M.E.R Shanahan, The influence of solid micro-deformation on contact angle equilibrium, J. Phys. D: Appl. Phys., 1987, **20**, 945-950

[32] A. Carré, J.C. Gastel, M.E.R. Shanahan, Viscoelastic effects in the spreading of liquids, Nature, 1996, **379**, 432-434

[33] R.W. Style, R. Boltyanskiy, Y. Che, J.S. Wettlaufer, L. Wilen, E.R. Dufresne, Universal deformation of soft substrates near a contact line an dthe direct measurement of solid surface stresses, Phys. Rev. Lett., 2013, **110**, 066103

[34] R.W. Style, A. Jagota, C.Y. Hui, E.R. Dufresne, Elastocapillarity: surface tension and the mechanics of soft solids, Ann. Rev. Condensed Matter Physics, 2017, **8**, 99-118

[35] L. Espın and S. Kumar, Droplet Spreading and Absorption on Rough, Permeable Substrates, J. Fluid Mech., 2015, **784**, 465-486

[36] Z. Wang, L. Espın, F. S. Bates, S. Kumar, and C. W. Macosko, Water Droplet Spreading and Imbibition on Superhydrophilic Poly(butylene terephthalate) Melt-blown Fiber Mats, Chem. Eng. Sci., 2016, **146**, 104-114

[37] S. Kumar and V. Charitatos, The Influence of Surface Roughness on Droplet Evaporation and Absorption: Insights into Experiments from Lubrication-Theory-Based Models, Langmuir, 2022, **38**, 15889-15904

[38] J. Crank, *The mathematics of diffusion*, Oxford Science Publication, Oxford, 197